DESIGN OF DISCRETE-TIME RIDE CONTROL SYSTEMS

L. Ding, A. Bradshaw and C. J. Taylor

Engineering Department, Lancaster University, UK, l.ding@email.com

Abstract: The paper presents the design of discrete-time Robust Inverse Dynamic Estimation (RIDE) control systems for an Advanced Gas-Cooled Reactor (AGR) of a nuclear power plant. Simulation experiments yield satisfactory transient responses for a linearised Multi-Input, Multi-Output (MIMO) state-space model, which is derived from a high-order non-linear industrial performance plant model.

Keywords: Discrete-time RIDE Controller, Digital Control

1. INTRODUCTION

Like many other branches of technology, the field of automatic control underwent rapid changes as a result of the increasing availability of first analogue and then digital computers. Current trends in control system theory reflect our ability to use analogue and, especially, digital computers to obtain numerical solutions to complex problems that do not admit analytical treatment. Furthermore, they admit the possibility of employing special purpose digital computers – as control system components – to process large amounts of data and / or implement complex control laws. The use of digital computers in these capacities is particularly natural in the case of systems that are discrete in nature, for example: (1) sampled-data systems, in which the data is sampled at discrete time instants, but the control signals are continuous; and (2) sequential systems, in which the control signals are input at discrete time instants. The common characteristic of sampled-data and sequential models is the discreteness of time. For this reason, they are referred to as discrete-time systems (Zadeh, 1968).

In this paper, a continuous-time Robust Inverse Dynamics Estimation (RIDE) control system (Bradshaw, *et al*., 1992; Muir, *et al*., 1996) is designed for the control of an Advanced Gas-Cooled Reactor (AGR) for a Nuclear Power Plant (Ding, 2003). The paper provides an introduction to the design of discrete-time RIDE control systems using digital computers and illustrates the transient responses for the linearised Multi-Input, Multi-Output (MIMO) state-space model (Kim, 1997) of an Advanced Gas-Cooled Reactor (AGR) Power Plant.

2. ADVANCED GAS-COOLED REACTOR

The AGR is an advance on the Magnox reactor. Magnox is the trade name of the magnesium alloy cladding around the natural uranium fuel of this type of reactor. The design of the AGR is unique in that the coolant of this type of reactor is carbon dioxide at a pressure of 40 bar and the outlet temperature of the gas is 650°C (Kim, 1997).

As shown in Fig. 1, the AGR has a graphite moderator, made up of large graphite bricks with channels for the fuel, control rods and pressured carbon dioxide (CO_2) coolant. In order for the reactors to function safely, the Advanced Gas-Cooled Reactor (AGR) is cased in a steel-lined pre-stressed concrete pressure vessel several metres thick which also acts as the biological shield, with the boilers inside. In the reactor core, nuclear fission produces tremendous heat. The CO_2 coolant passes through the reactor core, sends heat from the fission process to the boilers and is then re-circulated to the reactor core to be reheated. The turbine is directly coupled to an alternator to generate a nominal 660MW output. During this process there is no contact between the steam and the mildly radioactive CO_2 coolant or between the steam and the seawater used to cool it.

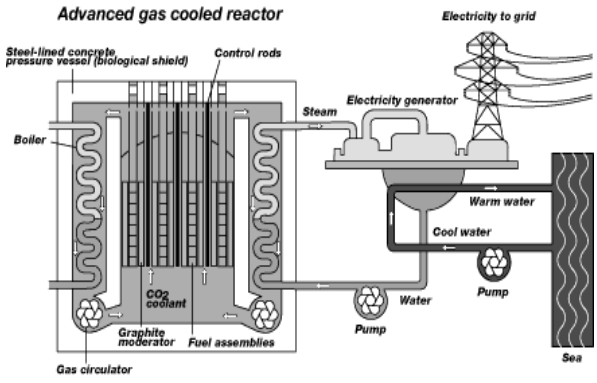

Figure 1 The AGR Power Station.

3. DISCRETE-TIME RIDE CONTROL SYSTEM

Discrete-time implementation of control systems are of importance since nearly all modern control systems are implemented on embedded microprocessors.

It is assumed that the plant can be described in vector-matrix form by the discrete-time state and output equations:

$$\boldsymbol{x}(k+1) = \boldsymbol{P}\boldsymbol{x}(k) + \boldsymbol{G}\boldsymbol{u}(k) \qquad (1)$$

and

$$\boldsymbol{y}(k) = \boldsymbol{H}\boldsymbol{x}(k) \qquad (2)$$

where $\boldsymbol{x}(k) \in \mathrm{R}^{n\times 1}$ is the plant state vector; $\boldsymbol{u}(k) \in \mathrm{R}^{m\times 1}$ is the plant input vector; $\boldsymbol{y}(k) \in \mathrm{R}^{m\times 1}$ is the plant output vector; $\boldsymbol{P} \in \mathrm{R}^{n\times n}$ is the plant state matrix; $\boldsymbol{G} \in \mathrm{R}^{n\times m}$ is the plant input matrix; and $\boldsymbol{H} \in \mathrm{R}^{m\times n}$ is the plant output matrix.

If a signal has discrete values e_0, e_1, …, e_k, … the z-transform of the signal can be defined as the function:

$$\boldsymbol{E}(z) \triangleq Z\{\boldsymbol{e}(k)\} \triangleq \sum_{k=-\infty}^{\infty} \boldsymbol{e}_k z^{-k} \qquad r_0 < |z| < R_0 \qquad (3)$$

and we assume that we can find values of r_0 and R_0 as bounds on the magnitude of the complex variable z for which the series equation (3) converges.

Using the above definition in the z-domain, the state and output equations (1) and (2) can be expressed in the forms:

$$(z-1)\boldsymbol{x}(z) = (\boldsymbol{P}-\boldsymbol{I})\boldsymbol{x}(z) + \boldsymbol{G}\boldsymbol{u}(z) \qquad (4)$$

and

$$\boldsymbol{y}(z) = \boldsymbol{H}\boldsymbol{x}(z) \qquad (5)$$

If the control input maintains $\boldsymbol{y}(k+1) - \boldsymbol{y}(k) = 0$, which means $(z - 1)\boldsymbol{y}(z) = 0$ in the z-domain, then the corresponding control term $\overline{\boldsymbol{u}}_{trim}(z)$ must satisfy the following equation:

$$-\boldsymbol{H}\boldsymbol{G}\overline{\boldsymbol{u}}_{trim}(z) = \boldsymbol{H}(\boldsymbol{P}-\boldsymbol{I})\boldsymbol{x}(z) \qquad (6)$$

Also, the state equation for the integral of error can be represented as follows:

$$\boldsymbol{w}(k+1) = \boldsymbol{w}(k) + [\boldsymbol{r}(k) - \boldsymbol{y}(k)] \qquad (7)$$

where $\boldsymbol{w}(k) \in \mathrm{R}^{m\times 1}$ is the integral of error; $\boldsymbol{r}(k) \in \mathrm{R}^{m\times 1}$ is the command input vector. Finally, equation (7) can be re-expressed in the z-domain as:

$$(z-1)\boldsymbol{w}(z) = \boldsymbol{r}(z) - \boldsymbol{y}(z) \qquad (8)$$

The block diagram of the discrete-time system with RIDE controller is shown in Fig. 2.

The theory of discrete-time RIDE control system design follows the same procedure as the continuous-time RIDE control system. The control law can be expressed in the form:

$$\boldsymbol{u}(k) = \overline{\boldsymbol{K}}_{\boldsymbol{I}}\boldsymbol{w}(k) - \overline{\boldsymbol{K}}_{\boldsymbol{P}}\boldsymbol{y}(k) + \hat{\overline{\boldsymbol{u}}}_{\boldsymbol{trim}}(k) \qquad (9)$$

where $\hat{\overline{\boldsymbol{u}}}_{trim}(k)$ is an estimate of the dynamic trim $\overline{\boldsymbol{u}}_{trim}(k)$; $\overline{\boldsymbol{K}}_{\boldsymbol{I}} \in \mathrm{R}^{m\times m}$ is the integral gain matrix; and $\overline{\boldsymbol{K}}_{\boldsymbol{P}} \in \mathrm{R}^{m\times m}$ is the proportional gain matrix. In the z-domain, equation (9) can be represented in the form:

$$\boldsymbol{u}(z) = \overline{\boldsymbol{K}}_{\boldsymbol{I}}\boldsymbol{w}(z) - \overline{\boldsymbol{K}}_{\boldsymbol{P}}\boldsymbol{y}(z) + \hat{\overline{\boldsymbol{u}}}_{\boldsymbol{trim}}(z) \qquad (10)$$

It is clear that equations (4) and (5) give:

$$(z-1)\boldsymbol{y}(z) = \boldsymbol{H}(\boldsymbol{P}-\boldsymbol{I})\boldsymbol{x}(z) + \boldsymbol{H}\boldsymbol{G}\boldsymbol{u}(z) \qquad (11)$$

Substituting equation (10) into equation (11) yields:

$$[(z-1)\boldsymbol{I} + \boldsymbol{H}\boldsymbol{G}\overline{\boldsymbol{K}}_{\boldsymbol{P}}]\boldsymbol{y}(z) = \boldsymbol{H}(\boldsymbol{P}-\boldsymbol{I})\boldsymbol{x}(z) + \boldsymbol{H}\boldsymbol{G}\overline{\boldsymbol{K}}_{\boldsymbol{I}}\boldsymbol{w}(z) + \boldsymbol{H}\boldsymbol{G}\hat{\overline{\boldsymbol{u}}}_{\boldsymbol{trim}}(z) \qquad (12)$$

and substituting equation (6) into equation (12) gives:

$$[(z-1)\boldsymbol{I} + \boldsymbol{H}\boldsymbol{G}\overline{\boldsymbol{K}}_{\boldsymbol{P}}]\boldsymbol{y}(z) = -\boldsymbol{H}\boldsymbol{G}\overline{\boldsymbol{u}}_{\boldsymbol{trim}}(z) + \boldsymbol{H}\boldsymbol{G}\overline{\boldsymbol{K}}_{\boldsymbol{I}}\boldsymbol{w}(z) + \boldsymbol{H}\boldsymbol{G}\hat{\overline{\boldsymbol{u}}}_{\boldsymbol{trim}}(z) \qquad (13)$$

so that equation (13) can be re-expressed as follows:

$$(z-1)[(z-1)\boldsymbol{I} + \boldsymbol{H}\boldsymbol{G}\overline{\boldsymbol{K}}_{\boldsymbol{P}}]\boldsymbol{y}(z) = \boldsymbol{H}\boldsymbol{G}[\overline{\boldsymbol{K}}_{\boldsymbol{I}}(z-1)\boldsymbol{w}(z) + (z-1)(\hat{\overline{\boldsymbol{u}}}_{\boldsymbol{trim}}(z) - \overline{\boldsymbol{u}}_{\boldsymbol{trim}}(z))] \qquad (14)$$

Substituting equation (8) into equation (14) leads to:

$$[(z-1)^2\boldsymbol{I} + (z-1)\boldsymbol{H}\boldsymbol{G}\overline{\boldsymbol{K}}_{\boldsymbol{P}} + \boldsymbol{H}\boldsymbol{G}\overline{\boldsymbol{K}}_{\boldsymbol{I}}]\boldsymbol{y}(z) = \boldsymbol{H}\boldsymbol{G}[\overline{\boldsymbol{K}}_{\boldsymbol{I}}\boldsymbol{r}(z) + (z-1)(\hat{\overline{\boldsymbol{u}}}_{\boldsymbol{trim}}(z) - \overline{\boldsymbol{u}}_{\boldsymbol{trim}}(z))] \qquad (15)$$

then the output vector of the discrete-time RIDE control system can be expressed in the z-domain:

$$\boldsymbol{y}(z) = [(z-1)^2\boldsymbol{I} + (z-1)\boldsymbol{H}\boldsymbol{G}\overline{\boldsymbol{K}}_{\boldsymbol{P}} + \boldsymbol{H}\boldsymbol{G}\overline{\boldsymbol{K}}_{\boldsymbol{I}}]^{-1} \boldsymbol{H}\boldsymbol{G}[\overline{\boldsymbol{K}}_{\boldsymbol{I}}\boldsymbol{r}(z) + (z-1)(\hat{\overline{\boldsymbol{u}}}_{\boldsymbol{trim}}(z) - \overline{\boldsymbol{u}}_{\boldsymbol{trim}}(z))] \qquad (16)$$

If the proportional gain matrix $\overline{\boldsymbol{K}}_{\boldsymbol{P}}$ is selected such that:

$$\overline{\boldsymbol{K}}_{\boldsymbol{P}} = (\boldsymbol{H}\boldsymbol{G})^{-1}\overline{\boldsymbol{\Sigma}} \qquad (17)$$

and the integral gain matrix $\overline{\boldsymbol{K}}_{\boldsymbol{I}}$ is selected such that:

$$\overline{\boldsymbol{K}}_{\boldsymbol{I}} = (\boldsymbol{H}\boldsymbol{G})^{-1}\overline{\boldsymbol{\Xi}} \qquad (18)$$

where it is assumed that $\boldsymbol{H}\boldsymbol{G}$ is non-singular, while $\overline{\boldsymbol{\Sigma}} \in \mathrm{R}^{m\times m}$ and $\overline{\boldsymbol{\Xi}} \in \mathrm{R}^{m\times m}$ are diagonal matrices. If $\boldsymbol{H}\boldsymbol{G}$ is singular then the feedback can be modified as in Porter, *et al.* (1981b). But this is not necessary for the applications covered in the present paper.

Substituting equations (17) and (18) into equation (16), the output equation in the z-domain for the closed-loop discrete-time control system will be:

$$\boldsymbol{y}(z) = [(z-1)^2\boldsymbol{I} + (z-1)\overline{\boldsymbol{\Sigma}} + \overline{\boldsymbol{\Xi}}]^{-1} [\overline{\boldsymbol{\Xi}}\boldsymbol{r}(z) + \boldsymbol{H}\boldsymbol{G}(z-1)(\hat{\overline{\boldsymbol{u}}}_{\boldsymbol{trim}}(z) - \overline{\boldsymbol{u}}_{\boldsymbol{trim}}(z))] \qquad (19)$$

If the estimate, $\hat{\overline{\boldsymbol{u}}}_{trim}(z)$, is good enough, the term in $(\hat{\overline{\boldsymbol{u}}}_{trim}(z) - \overline{\boldsymbol{u}}_{trim}(z))$ can be ignored, so that:

$$\boldsymbol{y}(z) = [(z-1)^2\boldsymbol{I} + (z-1)\overline{\boldsymbol{\Sigma}} + \overline{\boldsymbol{\Xi}}]^{-1}[\overline{\boldsymbol{\Xi}}\boldsymbol{r}(z)] \qquad (20)$$

As $\overline{\boldsymbol{\Sigma}}$ and $\overline{\boldsymbol{\Xi}}$ are both diagonal matrices, they can be described in the forms:

$$\overline{\boldsymbol{\Sigma}} = diag(\overline{\sigma}_1, \overline{\sigma}_2, ..., \overline{\sigma}_m) \qquad (21)$$

and

$$\overline{\boldsymbol{\Xi}} = diag(\overline{\rho}_1, \overline{\rho}_2, ..., \overline{\rho}_m) \qquad (22)$$

so that, in the z-domain, the closed-loop transfer matrix is diagonal, with the respective diagonal terms in the form:

$$G_i(z) = \frac{y_i(z)}{r_i(z)} = \frac{\overline{\rho}_i}{(z-1)^2 + \overline{\sigma}_i(z-1) + \overline{\rho}_i} \qquad (i = 1, 2, \ldots, m) \qquad (23)$$

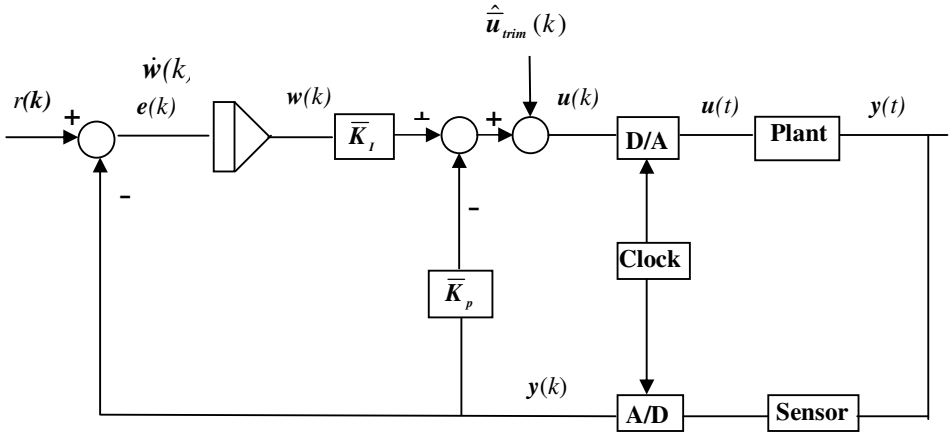

Figure 2 Block Diagram of the Discrete-Time System with RIDE Control.

and equation (23) can be re-expressed in the form:

$$G_i(z) = \frac{y_i(z)}{r_i(z)} = \frac{\bar{\rho}_i}{z^2 + (\bar{\sigma}_i - 2)z + (1 - \bar{\sigma}_i + \bar{\rho}_i)} \quad (i = 1, 2, \ldots, m) \quad (24)$$

Therefore, for the discrete-time RIDE control system, the input-output channels are de-coupled. The diagonal proportional gain tuning matrix, $\bar{\boldsymbol{\Sigma}}$, and the diagonal integral gain tuning matrix, $\bar{\boldsymbol{\Xi}}$, can be chosen to make all of the poles of the closed-loop control system lie inside the unit circle in the z-plane and thereby make the system stable. This paper considers the first application of the RIDE control law in the discrete-time case for a nonlinear high-order industrial performance plant model.

4. DISCRETE-TIME RIDE CONTROLLER IMPLEMENTATION

In this section, the RIDE controller design method is used to design a discrete-time control system for the linearised MIMO discrete-time state-space model of the AGR power plant. The corresponding time responses are obtained and analysed in the next section. It is thus shown that the RIDE controller design method can be implemented successfully for a linearised high-order industrial discrete-time system.

The linearised MIMO discrete-time state-space model can be derived from the continuous-time model (Ding, 2003) by using the MATLAB function *c2d*. The corresponding MATLAB programs were compiled. The linearised MIMO discrete-time state-space model was obtained and used to carry out the following simulation trials. A block diagram of the discrete-time RIDE controller implemented to the linearised MIMO discrete-time state-space model is constructed using the MATLAB/SIMULINK© package.

In this case, the system is a 3 input and 3 output high-order control system. The linearised state-space model has 21 state variables. So the matrices in equations (17) and (18) have the dimensions as follows: the input matrix $\boldsymbol{G} \in \mathrm{R}^{21\times3}$; the output matrix $\boldsymbol{H} \in \mathrm{R}^{3\times21}$; the proportional gain matrix $\bar{\boldsymbol{K}}_P \in \mathrm{R}^{3\times3}$; the integral gain matrix $\bar{\boldsymbol{K}}_I \in \mathrm{R}^{3\times3}$; and the diagonal gain matrices $\bar{\boldsymbol{\Sigma}} \in \mathrm{R}^{3\times3}$ and $\bar{\boldsymbol{\Xi}} \in \mathrm{R}^{3\times3}$.

It is worthwhile to note that, in order to protect the control system against overload, the three rate limiters are set in the three individual channels with the parameters shown in table 1.

Table 1 the Parameters of the Three Rate Limiters

Control Loops	Rate Limits	
	Rising Slew Rate	Falling Slew Rate
UTJ Temp. Control Loop	0.0108	-0.0108
HUVDP Control Loop	0.017	-0.017
TSVP Control Loop	0.025	-0.025

where UTJ stands for Unit-Boiler Transition Joint; HUVDP stands for the Half-Unit Valve Differential Pressure; and TSVP stands for Turbine Stop Valve Pressure.

In order to study the effect of the discretisation on the poles and zeros of the plant, the poles and zeros of the discrete-time state-space model are obtained by using the MATLAB functions *eig* and *zero* with the sample period T as 0.1 seconds.

The poles and zeros of the discrete-time state-space model can be compared with the poles and zeros of the continuous-time system (Ding, 2003). Poles close to zero in the z-plane are associated with dynamic modes that decay faster than those associated with poles closer to the circumference of the unit circle.

In this case, there is one pair of complex-conjugate poles and 19 real poles, together with three pairs of complex-conjugate zeros and 12 real zeros. It can be seen that they are all inside the unit circle of the z-plane

and the open-loop system is stable. Most importantly all the zeros are within the unit circle so that the closed-loop system will be stable even for a high gain.

In order to carry out the corresponding simulation trials, a suitable sample period T should be chosen to obtain satisfactory responses. Generally, the performance of a discrete-time control system improves with increasing sample rate (or decreasing sample period T), but the cost may also increase with faster sampling due to the requirement for faster computation power. So the selection of the best sample rate for a discrete-time control system is a compromise. A reasonable choice of T is one that results in at least 6 samples in the closed-loop rise time t_r, with smoother control results if there are more than 10 samples in the rise time t_r (Franklin, *et al.*, 1994). For the three control loops of the continuous-time RIDE control system (Ding, 2003), the fastest rise time t_r is 5.901 seconds in the second control loop. Therefore, the sample period T is initially chosen as 0.5 seconds.

For the continuous-time RIDE control system (Ding, 2003), the diagonal proportional gain matrix Σ and the diagonal integral gain matrix Ξ are obtained by the root loci of the closed-loop system and associated simulation trials (Ding, 2003). The diagonal proportional gain matrix Σ is obtained as follows:

$$\boldsymbol{\Sigma} = \begin{bmatrix} 0.02 & 0 & 0 \\ 0 & 0.2 & 0 \\ 0 & 0 & 0.2 \end{bmatrix} \qquad (25)$$

and the diagonal integral gain matrix $\boldsymbol{\Xi}$ is obtained as:

$$\boldsymbol{\Xi} = \begin{bmatrix} 0.0001 & 0 & 0 \\ 0 & 1 & 0 \\ 0 & 0 & 0.1 \end{bmatrix} \qquad (26)$$

Firstly, the simulation trials were carried out with the linearised MIMO discrete-time simulation model by using the same parameters of $\boldsymbol{\Sigma}$ and $\boldsymbol{\Xi}$ shown in equations (25) and (26). A -5°C step change in the Unit-Boiler Transition Joint (UTJ) temperature reference; a +1 bar step change in the Half-Unit Valve Differential Pressure (HUVDP) reference; and a +5 bar step change in the Turbine Stop Valve Pressure (TSVP) reference were chosen individually to analyse the corresponding time response behaviour. These are obtained using SIMULINK, with the results illustrated in Fig. 3, Fig. 4 and Fig. 5.

In order to improve the performance of the discrete-time RIDE control system, the sample period T is decreased to 0.1 seconds. The simulation trials were carried out again by using the same parameters shown in equations (25) and (26). Due to the effect of the rate limiters, high frequency oscillations occurred after a +1 bar step change was input in the HUVDP reference. For the continuous-time RIDE control system (Ding, 2003), if the rise time t_r of the closed-loop system is too fast, the integral gain matrix $\boldsymbol{\Xi}$ needs to be decreased to increase the value of the rise time t_r of the closed-loop system, in order to slow down the speed of the time responses. The relationship between the rise time t_r and the diagonal integral gain matrix $\boldsymbol{\Xi} = \text{diag}(\rho_1, \rho_2, \ldots, \rho_m)$ is shown as follows (Ding, 2003):

$$t_{rj} \cong \frac{1.8}{\sqrt{\rho_j}} \qquad (27)$$

This relationship also applies equally well to the discrete-time RIDE control system. So for the second control loop (HUVDP), after decreasing the second element $\bar{\rho}_2$ of the diagonal integral gain matrix $\overline{\boldsymbol{\Xi}}$ from 1 to 0.1, the simulation trials were carried out again and the high frequency oscillations were eliminated as expected.

Therefore, for the discrete-time RIDE control system, the sample period T is chosen as 0.1 seconds and the diagonal proportional gain matrix $\overline{\boldsymbol{\Sigma}}$ is kept the same as $\boldsymbol{\Sigma}$ shown in equation (25) and set as follows:

$$\overline{\boldsymbol{\Sigma}} = \begin{bmatrix} 0.02 & 0 & 0 \\ 0 & 0.2 & 0 \\ 0 & 0 & 0.2 \end{bmatrix} \qquad (28)$$

and the diagonal integral gain matrix $\overline{\boldsymbol{\Xi}}$ is set as:

$$\overline{\boldsymbol{\Xi}} = \begin{bmatrix} 0.0001 & 0 & 0 \\ 0 & 0.1 & 0 \\ 0 & 0 & 0.1 \end{bmatrix} \qquad (29)$$

The proportional gain matrix $\overline{\boldsymbol{K}}_P$ and the integral gain matrix $\overline{\boldsymbol{K}}_I$ can be obtained by substituting equations (28) and (29) into equations (17) and (18) individually.

By following this procedure, satisfactory parameters were obtained for the discrete-time RIDE control system with the rate limiters in the three individual control loops. The simulation results are presented and discussed in the next section.

5. SIMULATION RESULTS

Using the values of the proportional gain matrix $\overline{\boldsymbol{K}}_P$ and the integral gain matrix $\overline{\boldsymbol{K}}_I$ obtained above, the following simulation trials were carried out for the linearised MIMO discrete-time RIDE control system model. For the discrete-time RIDE control system, the step change is divided by the sampling period T, to give a rate which will be limited by the rising slew rate and the falling slew rate of the rate limiters, whilst still maintaining system safety.

The three step changes were chosen individually to analyse the corresponding time response behaviour. Firstly, by inputting a -5°C step change in the UTJ temperature reference, the corresponding time responses are obtained by SIMULINK and illustrated in Fig. 6.

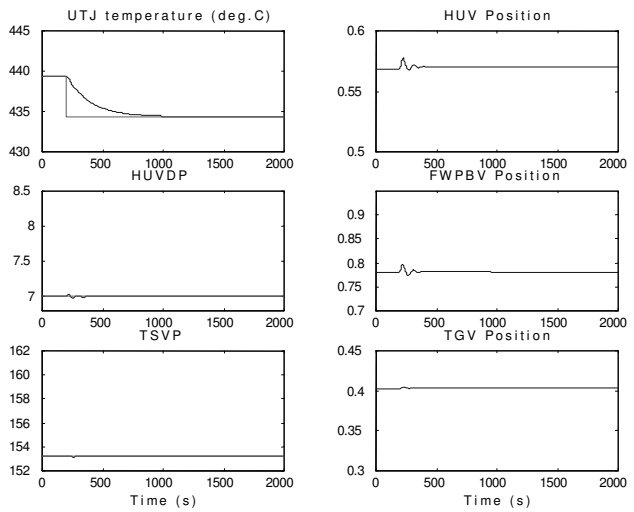

Figure 3 Time responses with a -5°C step change in the UTJ temperature reference.

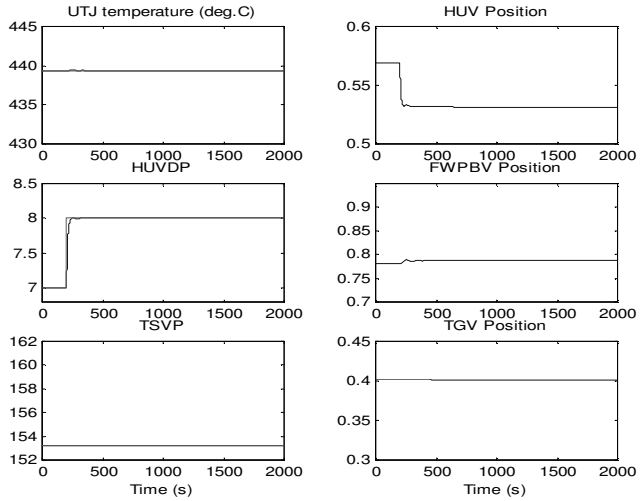

Figure 4 Time responses with a +1 bar step change in the HUVDP reference.

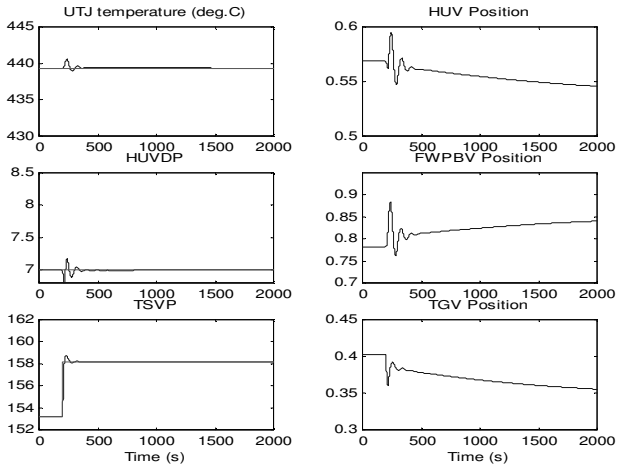

Figure 5 Time responses with a +5 bar step change in the TSVP reference.

It can be seen that the closed-loop system has a satisfactory behaviour after inputting a -5°C step change in the UTJ temperature reference, i.e. less oscillations and the speed of the responses is fairly fast. These simulation results can be compared with the corresponding time responses of the continuous-time RIDE control system (Ding, 2003). It is clear that for the HUV position $\boldsymbol{u_1(t)}$ and the FWPBV position $\boldsymbol{u_2(t)}$, the speed of the time responses is increased and the oscillations are decreased. So we can say that the time responses of the discrete-time RIDE control system are slightly improved over the continuous-time RIDE control system, for the same command input in the UTJ temperature reference.

For the HUVDP control loop, a +1 bar step change is input in the HUVDP reference, with the corresponding time responses obtained and illustrated in Fig. 7. The time responses also show satisfactory behaviour for a +1 bar step change in the HUVDP reference. The output variable $\boldsymbol{y_2(t)}$ of the HUVDP control loop is driven towards the required steady-state value and the speed of the response is fairly fast. The simulation results shown in Fig. 7 can also be compared with the corresponding time responses of the continuous-time RIDE control system (Ding, 2003). It can be noted that the time responses of the discrete-time RIDE control system have fewer oscillations than those of the continuous-time RIDE control system and the behaviour is also slightly improved.

Following the same procedure, a +5 bar step change is input in the TSVP reference, with the time responses illustrated in Fig. 8. For this reference input, the output variable $\boldsymbol{y_3(t)}$ of the TSVP control loop is driven towards the required steady-state value and the speed of the response is also fairly fast. It can be seen that the speed of the time responses in Fig. 8 is speeded up and the time responses have fewer oscillations and lower overshoots than the corresponding time responses with the continuous-time RIDE controller (Ding, 2003). Hence, we can also say that the time response behaviour is improved with the discrete-time RIDE controller.

6. CONCLUSIONS

This paper investigates a discrete-time approach to Robust Inverse Dynamic Estimation (RIDE) control (Bradshaw, *et al*., 1992; Muir, *et al*., 1996), applied to a linearized 3-input, 3-output state-space model of a nuclear power plant. The latter system has been derived from a high-order industrial non-linear performance plant model for an Advanced Gas-Cooled Reactor (AGR) power plant. Simulation experiments are carried out to help obtain satisfactory parameters for the proportional gain matrix $\overline{\boldsymbol{K}}_P$ and the integral gain matrix $\overline{\boldsymbol{K}}_I$. The time responses of the resulting closed-loop control system are compared with the corresponding time responses of the continuous-time RIDE control system (Ding, 2003).

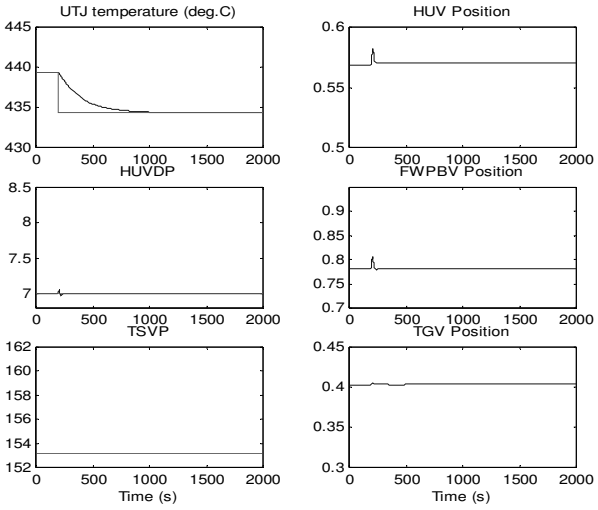

Figure 6 Time responses with a -5°C step change in the UTJ temperature reference with new parameters.

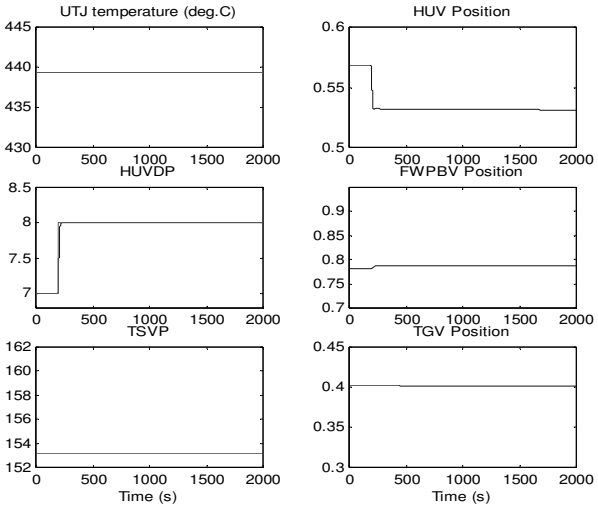

Figure 7 Time responses with a +1 bar step change in the HUVDP reference with new parameters.

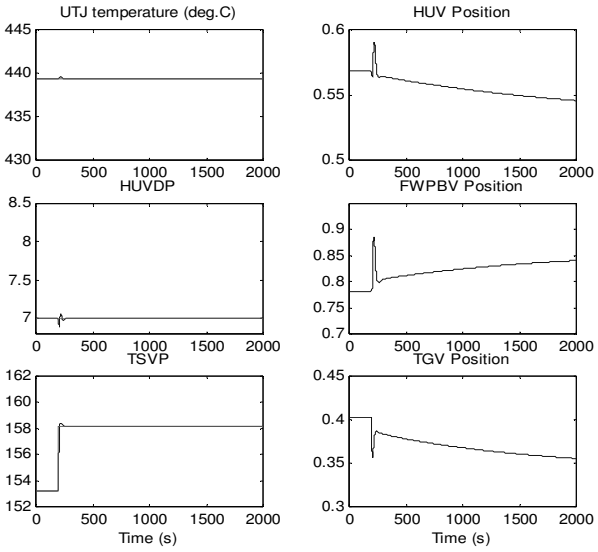

Figure 8 Time responses with a +5 bar step change in the TSVP reference with new parameters.

The discrete-time RIDE control system is found to yield improved performance in comparison to the continuous-time equivalent previously developed. This unexpected result is probably associated with the non-linearities introduced by the rate limiters, although the reasons for this require further research. However, the simulation experiments also show that the discrete-time algorithm requires careful selection the sample period T in order to obtain satisfactory results.

It should be noted that non-linear blocks for the rate limiters are installed for all three channels of the control system. This ensures that the plant variables stay within the range of validity of the linearised model during all the simulation trials. In the case of large amplitude commands, it is necessary to use a number of linear models to schedule the controller gains according to the particular amplitude of the variables. This is the approach that will be used in the control of the full non-linear system, a subject of future research.

However, to the authors knowledge, the present paper represents the first time that the discrete-time RIDE control system has been successfully applied to a high-order industrial control system simulation.

REFERENCES

Bradshaw, A. and J.M. Counsell (1992). Design of Autopilots for High Performance Missiles, *Proc. Instn. Mech. Engrs., Journal of Systems and Control*, **206**, 75-84.

Ding, L. (2003). *Comparison of Some New Schemes for the Control of the Boiler of a Nuclear Power Plant*, Doctoral Thesis, Lancaster University, Lancaster, LA1 4YR.

Franklin, G.F., J.D. Powell and A. Emami-Naeini (1994). *Feedback control of dynamic systems - third edition*. Addison-Wesley Publishing Company, Inc.

Kim, H.J. (1997). *Robustness analysis and development of a boiler control system for an Advanced Gas-Cooled Reactor Power Station*, MSc. Diss., Lancaster University, Lancaster LA1 4YR.

Muir, E. and A. Bradshaw (1996). Control Law Design for a Thrust Vectoring Fighter Aircraft Using Robust Inverse Dynamics Estimation (RIDE), *Proc. Instn. Mech. Engrs., Part G, Journal of Aerospace Engineering*, **210(G)**, 333-343.

Porter, B. and A. Bradshaw (1981b), Singular Perturbation Methods in the Design of Tracking Systems Incorporating Inner-Loop Compensators, *International Journal of Systems Science*, **12(10)**, 1193-1205.

Zadeh, L.A. (1968). Computing Methods in Optimisation Problems 2, *Papers Presented at a Conference Held* at San Remo, Italy, Sept. 9-13.